Noncoherent Symbol Synchronization Techniques[1]

Marvin Simon
Jet Propulsion Laboratory, California Institute of Technology

Abstract- Traditional methods for establishing symbol synchronization (sync) in digital communication receivers assume that carrier sync has already been established, i.e., the problem is addressed at the baseband level assuming that a "perfect" estimate of carrier phase is available. We refer to this approach as *coherent symbol sync*. Since, for NRZ signaling, a suppressed carrier sync loop such as an I-Q Costas loop includes integrate-and-dump (I&D) filters in its in-phase (I) and quadrature (Q) arms, the traditional approach is to first track the carrier in the absence of symbol sync information, then feed back the symbol sync estimate to these filters, and then iterate between the two to a desirable operating level. In this paper, we revisit the symbol sync problem by examining methods for obtaining such sync in the absence of carrier phase information, i.e., so-called *noncoherent symbol sync loops*. We compare the performance of these loops with that of a well-known coherent symbol sync loop and examine the conditions under which one is preferable over the other.

1. Introduction

The operation and performance of various functions of a digital communication receiver can be quite sensitive to knowledge of the timing (data transition epochs) of the received data symbols. Thus, the ability to accurately estimate this parameter and continuously update the estimate, i.e., perform *symbol synchronization (sync)*, is critical to successful operation of such a receiver. Traditionally, symbol sync techniques have been developed assuming that the data symbols are binary, the modulation format, e.g., NRZ or Manchester data, is known a priori, and carrier sync is perfect. As such, the symbol sync problem has been solved entirely at baseband assuming perfect knowledge of the carrier phase and frequency. In what follows it will be convenient to refer to the class of symbol synchronizers that result from such assumptions as *phase-coherent symbol synchronizers*. While in theory these ideal assumptions allow for readily developing open and closed loop symbol sync schemes based on maximum a posteriori (MAP) estimation principles, in practice these same assumptions are somewhat inappropriate. For example, the most commonly used suppressed-carrier sync scheme, i.e., the inphase-quadrature (I-Q) Costas loop, contains matched filters in its I and Q arms (which for NRZ data take form of integrate-and-dump (I&D) filters) whose implementation depends on knowledge of the symbol timing. Thus, in establishing both carrier and symbol sync one is faced with the "chicken and egg" problem as to which to perform first. The common means for handling this problem is to *first* obtain a degraded estimate of carrier sync assuming no knowledge of symbol sync[2] and then proceed to

---

[1] This work was performed at the Jet Propulsion Laboratory, California Institute of Technology under a contract with the National Aeronautics and Space Administration.

[2] The ability to obtain carrier sync prior to symbol sync is afforded by the possibility of successfully operating a Costas loop with I&D arm filters which, even in the worst case of a symbol sync error equal to one-half a data symbol time interval, still provides an estimate of carrier phase albeit at an increased mean-square phase error. On the contrary, a conventional symbol sync scheme cannot guarantee performing its function in the absence of carrier phase knowledge, particularly in the worst case of a phase error equal to $\pi/2$ radians. More about this shortly.

obtain symbol sync based on this carrier sync estimate. The symbol sync estimate is then fed back to the carrier synchronizer to improve its estimate whereupon the two sync functions continue to iterate with each other until a desired level of performance is reached.

Among the various phase-coherent symbol sync schemes that have been proposed in the literature, by far the most popular in terms of its application in binary communication systems is the *data transition tracking loop (DTTL)* [1,2]. The scheme as originally proposed in the late 1960s is an inphase-quadrature (I-Q) structure where the I arm produces a signal representing the polarity of a data transition (i.e., a comparison of hard (±1) decisions on two successive symbols) and the Q arm output is a signal whose absolute value is proportional to the timing error between the received signal epoch and the receiver's estimate of it. The result of the product of the I and Q signals is an error signal which is proportional to this timing error, independent of the direction of the transition. Although originally introduced as an efficient symbol synchronization means for tracking an NRZ data signal received in additive white Gaussian noise (AWGN), it was later demonstrated by the author (although not formally published) that the closed loop DTTL structure can be obtained from a suitable interpretation of the maximum a posteriori (MAP) open loop estimate of symbol timing based on an observation of say N symbols at high symbol signal-to-noise ratio (SNR).

At the time of its introduction in the late 1960's, the binary communication systems in which the DTTL was employed were for the most part uncoded and thus high symbol SNR was the region of primary interest. As time marched on, the design of communication systems became more and more power efficient through the application of error correction coding, and as such a greater and greater demand was placed on the symbol synchronizer which now had to operate in a low symbol[3] SNR region, with values based on today's coding technology perhaps as low as -8 dB. Since in this very low symbol SNR region, the DTTL scheme as originally proposed would no longer be the one motivated by MAP estimation theory, it is also likely that its tracking capability would be seriously degraded in this region of operation. Despite this fact, the conventional DTTL appears to have continued to be used in coded communication applications.

An alternative approach to phase-coherent symbol sync, which has particular application in so-called *autonomous receivers* where it is desired for the receiver to perform each of its functions *automonously*, i.e., with as little information of the others as possible, is *noncoherent symbol sync*. As mentioned in an earlier footnote, the conventional symbol sync schemes are not intended for such operation and thus, in general, could fail under such conditions. In this paper, we consider a class of well-known, albeit ad hoc, symbol synchronizers that by their very own construction naturally lend themself to modification so as to operate in the absence of carrier phase information. The mean-square tracking performance of these noncoherent symbol synchronizers will be presented and compared with that of their coherent counterparts. as well as that of the phase-coherent DTTL. Depending on the so-called "window width" of the DTTL, it will be demonstrated that these ad hoc noncoherent symbol synchronizers can become quite competitive or even superior performance-wise. With this in mind, one might then consider reversing the conventional order of obtaining sync as alluded to above at the same time eliminating altogether the need for iteration between the carrier and sync functions.

---

[3] It is important to note here that in a coded communication system, the symbol synchronizer precedes the decoder and thus performs its function on the *coded* symbols whose SNR is equal to the bit SNR times the code rate.

2. Symbol Synchronization in the Absence of Carrier Phase Information

In addition to "optimum" phase-coherent symbol synchronizers, such as the ones mentioned above that are motivated by the MAP estimation approach, several other suboptimum schemes have been proposed in the literature that offer the advantage of a simpler implementation and at the same time perform nearly as well as the more complex optimum ones. One of the more popular of these ad hoc schemes that draws its roots from the squaring loop used for carrier synchronization is called the *filter and square symbol synchronizer* whose tracking performance was analyzed in Ref. 3 explicitly for the case of an NRZ input and a single-pole Butterworth low pass filter for $H(s)$ (see Fig. 1). The operation of this scheme is briefly summarized as follows. The input binary data stream plus noise is first low pass filtered and then squared (with the purpose of removing the data information). The signal component of the output of the square-law contains a line spectrum with discrete components at integer multiples of the data rate $1/T$. Thus, following this signal with a zonal filter (to extract say the nth harmonic) a sinusoidal tone is generated at $f = n/T$ that can be tracked by a phase-locked loop (PLL) whose voltage-controlled oscillator (VCO) output after frequency division by n and an appropriate phase shift[4] represents a symbol timing clock that is synchronous with the input data stream.

Subsequent to the analysis of the filter and square symbol synchronizer reported in Ref. 3, a generalization of this scheme was introduced in Ref. 4 which did nothing more than replace the square-law device with a delay-and-multiply operation (see Fig. 2). The resulting configuration referred to as a *cross-spectrum symbol synchronizer* allowed, in general, for a delay element equal to a fraction α of the symbol time where the value of α would be chosen to optimize the tracking performance in the sense of minimizing the mean-square timing error. It is clear from a comparison of Figs. 1 and 2 that the filter and square law symbol synchronizer is a special case of the cross-spectrum symbol synchronizer corresponding to $\alpha = 0$. Once again assuming a single-pole Butterworth low pass filter for $H(s)$, the line spectrum at the output of the delay-and-multiply operation was analyzed in Ref. 4 as a function of the fractional delay α for both low and high SNRs. In particular, for a given value of SNR and α, it was shown that there exists an optimum filter bandwidth to data rate ratio[5] in the sense of minimizing the mean-square timing error and that the optimum value of α is in each case was equal to $1/2$. Furthermore, in addition to $\alpha = 1/2$ optimizing the performance for the best choice of filter bandwidth to data rate ratio, it also resulted in a significant improvement in robustness with regard to variations in this ratio.

While the filter and square symbol synchronizer and its generalization the cross-spectrum symbol synchronizer were initially proposed as real baseband schemes that implicitly assumed perfect carrier synchronization, it is straightforward to modify them so as to be useful in a phase-noncoherent mode. Specifically, if we model the signal component of the input in complex form as

$$\tilde{s}(t,\varepsilon) = \sqrt{2P}e^{j\theta_c}m(t), \quad m(t) = \sum_{n=-\infty}^{\infty} d_n p(t - nT - \varepsilon) \tag{1}$$

---

[4] The phase shifter is required to cancel the known phase shift inherent in the nth harmonic of the Fourier series representation of the signal component in the output of the of the squaring device.

[5] This phenomenon is entirely synergistic with the tracking performance of the Costas or squaring loop as exemplified by its squaring loss behavior as a function of the ratio of arm filter bandwidth to data rate ratio.

where P denotes the signal power, θ_c denotes the unknown carrier phase, $\{d_n\}$ is a binary independent and identically distributed (i.i.d.) data stream with equiprobable ±1 levels, $p(t)$ is a unit rectangular pulse of duration T, and ε is the unknown symbol timing, then performing the delay-and-multiply function in complex conjugate form will again result in a zonal filter output that is a tone at the nth harmonic of the data rate that can be tracked by a PLL. Furthermore, the performance of this scheme will be independent of the value of θ_c. A block diagram of the real noncoherent version of the cross-spectrum synchronizer is illustrated in Fig. 3 where the input is now the *bandpass* received signal whose signal component is given by $s(t,\varepsilon)=\mathrm{Re}\{\tilde{s}(t,\varepsilon)e^{j\omega_c t}\}$ with ω_c denoting the carrier frequency. In what follows we present the tracking performance of the symbol synchronizer in Fig. 3 drawing heavily on the detailed results already contained in Refs. 3 and 4.

In accordance with the above, the received bandpass signal is given by

$$\begin{aligned} r(t) &= s(t,\varepsilon)+n(t) \\ &= \sqrt{2P}m(t)\cos(\omega_c t+\theta_c)+\sqrt{2}\left[N_c(t)\cos\omega_c t - N_c(t)\sin\omega_c t\right] \end{aligned} \tag{2}$$

where $N_c(t), N_s(t)$ are independent low pass Gaussian noise processes with single-sided power spectral density N_0 w/Hz. After demodulation with quadrature reference signals

$$r_c(t)=\sqrt{2}\cos\omega_c t, \quad r_s(t)=-\sqrt{2}\sin\omega_c t \tag{3}$$

and then filtering and delay and multiplying, we obtain the I and Q low pass signals

$$\begin{aligned} \hat{x}_c(t) &= P\hat{m}(t)\hat{m}(t-\alpha T)\cos^2\theta_c + \hat{N}_c(t)\hat{N}_c(t-\alpha T) \\ &\quad +\sqrt{P}\cos\theta_c\left[\hat{m}(t)\hat{N}_c(t-\alpha T)+\hat{m}(t-\alpha T)\hat{N}_c(t)\right] \\ \hat{x}_s(t) &= P\hat{m}(t)\hat{m}(t-\alpha T)\sin^2\theta_c + \hat{N}_s(t)\hat{N}_s(t-\alpha T) \\ &\quad +\sqrt{P}\sin\theta_c\left[\hat{m}(t)\hat{N}_s(t-\alpha T)+\hat{m}(t-\alpha T)\hat{N}_s(t)\right] \end{aligned} \tag{4}$$

Summing these I and Q signals produces

$$\begin{aligned} x(t) &= P\hat{m}(t)\hat{m}(t-\alpha T)+\hat{N}_c(t)\hat{N}_c(t-\alpha T)+\hat{N}_s(t)\hat{N}_s(t-\alpha T) \\ &\quad +\sqrt{P}\hat{m}(t)\left[\hat{N}_c(t-\alpha T)\cos\theta_c+\hat{N}_s(t-\alpha T)\sin\theta_c\right] \\ &\quad +\sqrt{P}\hat{m}(t-\alpha T)\left[\hat{N}_c(t)\cos\theta_c+\hat{N}_s(t)\sin\theta_c\right] \end{aligned} \tag{5}$$

whose signal × signal ($S\times S$) component (the first term on the right hand side of (5)) is identical to that of the phase coherent cross-spectral symbol synchronizer and as such is independent of the carrier phase. It now remains to investigate to what extent the noise × noise ($N\times N$) component (the 2nd and 3rd terms on the right hand side of (5)) and the signal × noise ($S\times N$) component (the 4th and 5th terms on the right hand side of (5)) have changed and what impact these changes have on the tracking performance of the loop.

As is typical of all synchronization loops of this type, the tracking performance as measured by the normalized mean-square timing error $\sigma_\lambda^2 = E\left\{\left[\left(\varepsilon-\hat{\varepsilon}\right)/T\right]^2\right\}$, can be

characterized by the "squaring loss" which represents the degradation[6] in this measure due to the nonlinear nature ($S\times S$, $S\times N$ and $N\times N$ operations) of the loop. Specifically, the squaring loss is formed from a scaled version of the ratio of the power in the $S\times S$ component to the equivalent noise power spectral density of the sum of the $S\times N$ and $N\times N$ components all evaluated at the nth harmonic of the data rate. As we shall see shortly, it will not be necessary to redo the evaluations of these component contributions to the squaring loss from what was done in Refs. 3 and 4 for the phase-coherent symbol synchronizer. Rather, we shall simply be able to make direct use of the evaluations found there with simple or no modification at all. As such the evaluation of the squaring loss itself will follow immediately almost by inspection.

To evaluate the equivalent noise power spectral densities of the $S\times N$ and $N\times N$ components, namely, $N'_{0_{S\times N}}$ and $N'_{0_{N\times N}}$, respectively, we must first compute their autocorrelation function. The autocorrelation of the $S\times N$ component is by definition

$$\begin{aligned}
R_{sn}(\tau) &= PE\Big\{\Big[\hat{m}(t)\Big[\hat{N}_c(t-\alpha T)\cos\theta_c + \hat{N}_s(t-\alpha T)\sin\theta_c\Big] \\
&\quad +\hat{m}(t-\alpha T)\Big[\hat{N}_c(t)\cos\theta_c + \hat{N}_s(t)\sin\theta_c\Big]\Big] \\
&\quad \times\Big[\hat{m}(t+\tau)\Big[\hat{N}_c(t-\alpha T+\tau)\cos\theta_c + \hat{N}_s(t-\alpha T+\tau)\sin\theta_c\Big] \\
&\quad +\hat{m}(t-\alpha T+\tau)\Big[\hat{N}_c(t+\tau)\cos\theta_c + \hat{N}_s(t+\tau)\sin\theta_c\Big]\Big]\Big\} \qquad (6)\hat{} \\
&= 2PR_{\hat{m}}(\tau)\Big[R_{\hat{N}_c}(\tau)\cos^2\theta_c + R_{\hat{N}_s}(\tau)\sin^2\theta_c\Big] \\
&\quad +PR_{\hat{m}}(\tau+\alpha T)\Big[R_{\hat{N}_c}(\tau-\alpha T)\cos^2\theta_c + R_{\hat{N}_s}(\tau-\alpha T)\sin^2\theta_c\Big] \\
&\quad +PR_{\hat{m}}(\tau-\alpha T)\Big[R_{\hat{N}_c}(\tau+\alpha T)\cos^2\theta_c + R_{\hat{N}_s}(\tau+\alpha T)\sin^2\theta_c\Big]
\end{aligned}$$

which after recognizing that $R_{\hat{N}_c}(\tau) = R_{\hat{N}_s}(\tau) = R_{\hat{N}}(\tau)$ simplifies to

---

[6] As we shall see shortly, the "squaring loss" can at times exceed 0 dB and thus, in reality, represent a gain rather than a loss. The reason for using such a nomenclature here nonetheless is by analogy with its usage in the carrier sync application where it represents the additional degradation of the mean-square *phase* error relative to that of a linear carrier tracking loop such as a phase-locked loop (PLL) and hence its value there can never exceed 0 dB. The difference between the two usages is centered around the fact that in the carrier sync application the phase error can vary over a range of 2π rad. whereas in the symbol sync application the normalized (to the T-sec symbol duration) timing error can vary over a range of unity. Thus, there is a scale factor of $(2\pi)^2$ that comes into play when relating the mean-square phase error of the sinusoidal clock supplied by the PLL portion of the cross-spectrum symbol synchronizer to the mean-square timing error of this same reference when used as a symbol sync clock. The important point to keep in mind is that the "squaring loss" is just a relative measure of performance and thus useful in comparing different sync schemes.

$$R_{sn}(\tau) = P\left[2R_{\hat{m}}(\tau)R_{\hat{N}}(\tau) + R_{\hat{m}}(\tau+\alpha T)R_{\hat{N}}(\tau-\alpha T) + R_{\hat{m}}(\tau-\alpha T)R_{\hat{N}}(\tau+\alpha T)\right] \tag{7}$$

Again it can be observed that the autocorrelation in (7) is independent of the carrier phase θ_c and furthermore is identical to the analogous result for the phase-coherent cross-spectrum symbol synchronizer as given in Eq. (10) of Ref. 4.[7]

Next, the autocorrelation of the $N \times N$ component is obtained as

$$\begin{aligned} R_{nn}(\tau) &= E\left\{\left[\hat{N}_c(t)\hat{N}_c(t-\alpha T) + \hat{N}_s(t)\hat{N}_s(t-\alpha T)\right]\right. \\ &\quad \left.\times\left[\hat{N}_c(t+\tau)\hat{N}_c(t-\alpha T+\tau) + \hat{N}_s(t+\tau)\hat{N}_s(t-\alpha T+\tau)\right]\right\} \\ &= 2\left[R_{\hat{N}}^2(\alpha T) + R_{\hat{N}}^2(\tau) + R_{\hat{N}}(\tau-\alpha T)R_{\hat{N}}(\tau+\alpha T)\right] \end{aligned} \tag{8}$$

which is exactly twice the analogous result for the phase-coherent cross-spectrum symbol synchronizer as given in Ref. 4. Thus, since the equivalent noise power spectral densities are computed from the Fourier transforms of the autocorrelations evaluated at the nth harmonic of the data rate, i.e., $N'_{0_{S\times N}} = 2\int_{-\infty}^{\infty} R_{sn}(\tau)e^{j2\pi n\tau/T}d\tau$ and $N'_{0_{N\times N}} = 2\int_{-\infty}^{\infty} R_{nn}(\tau)e^{j2\pi n\tau/T}d\tau$, then ignoring the dc term $R_N^2(\alpha T)$ as was done in Ref. 4 (since it leads to a power spectral line component at zeroth harmonic of the data rate which is eliminated by the zonal filter), we conclude that

$$\begin{aligned} N'_{0_{S\times N}}\big|_{noncoh.} &= N'_{0_{S\times N}}\big|_{coh.} \\ N'_{0_{N\times N}}\big|_{noncoh.} &= 2N'_{0_{N\times N}}\big|_{coh.} \end{aligned} \tag{9}$$

Finally, since, as previously stated, the $S \times S$ component of the noncoherent cross-spectral symbol synchronizer is identical to that of the phase coherent one, then letting $|C_n|^2$ denote the normalized power in this component at the nth harmonic of the data rate, the squaring loss of the former is obtained as (see Eq. (49) of Ref. 4 with minor corrections applied)

$$\begin{aligned} S_L\big|_{noncoh.} &= (2\pi n)^2 PN_0\left[\frac{2|C_n|^2\big|_{noncoh.}}{N'_{0_{S\times N}}\big|_{noncoh.} + N'_{0_{N\times N}}\big|_{noncoh.}}\right] \\ &= (2\pi n)^2 PN_0\left[\frac{2|C_n|^2\big|_{coh.}}{N'_{0_{S\times N}}\big|_{coh.} + 2N'_{0_{N\times N}}\big|_{coh.}}\right] \end{aligned} \tag{10}$$

At this point it is straightforward to evaluate (10) by making use of the expressions in Ref. 4 for $|C_n|^2\big|_{coh.}$, $N'_{0_{S\times N}}\big|_{coh.}$ and $N'_{0_{N\times N}}\big|_{coh.}$. A summary of these results for the special case of a single pole Butterworth low pass filter for $H(s)$ (with 3 dB cutoff frequency f_c),

[7] Note that the multiplicative factor P has been included here in the definition of $R_{sn}(\tau)$ whereas in Ref. 4, where P is denoted by S, it has been erroneously omitted in defining the total noise power spectral density.

random (transition density equal to 0.5) NRZ data, n=1 (tracking of the first harmonic) and either $\alpha = 0$ (the filter and square law implementation) or $\alpha = 0.5$ (a half-symbol delay which was shown in Ref. 4 to be optimum in the sense of minimizing the squaring loss at the best ratio of low pass filter bandwidth to symbol time) are given below:[8]

$\underline{\alpha = 0}$

$$|C_1|^2 = \frac{[1-\exp(-2\pi R)]^2}{(2\pi R)^2}\frac{1}{[1+1/R^2][1+1/4R^2]}$$

$$N'_{0_{S\times N}}\Big|_{coh.} = \frac{4PN_0}{1+1/R^2}\left\{1-\frac{1-\exp(-2\pi R)}{8\pi R}\left[\frac{6+1/R^2+1/R^4}{[1+1/R^2][1+1/4R^2]}\right]\right\} \tag{11}$$

$$N'_{0_{N\times N}}\Big|_{coh.} = \frac{PN_0}{1+1/4R^2}\left(\frac{\pi R}{2E_s/N_0}\right)$$

$\underline{\alpha = 0.5}$

$$|C_1|^2 = \frac{1}{(2\pi)^2[1+1/R^2][1+1/4R^2]}\left\{\frac{[\exp(-\pi R)[3-\exp(-2\pi R)]-2]^2}{4R^2}+4\right\}$$

$$N'_{0_{S\times N}}\Big|_{coh.} = \frac{2PN_0}{1+1/R^2}\left\{1-\frac{1}{4\pi R}\left[\frac{1-1/R^2}{1+1/R^2}\right.\right.$$

$$\left.\left.+\frac{1}{2}\left(\frac{1+1/R^2}{1+1/4R^2}\right)\right](3-4\exp(-2\pi R)+\exp(-4\pi R))\right\} \tag{12}$$

$$N'_{0_{N\times N}}\Big|_{coh.} = \frac{PN_0}{1+1/4R^2}\left(\frac{\pi R}{4E_s/N_0}\right)[1-\exp(-2\pi R)]$$

where $R \triangleq f_c T$ and $E_s = PT$ is the symbol energy.

Fig. 4 is an illustration of $S_L|_{noncoh.}$ as computed from (10) together with (11) or (12) versus R with E_s/N_0 as a parameter. Also shown in dashed lines are the corresponding plots of the squaring loss performance for the coherent cross-spectrum symbol synchronizer, namely $S_L|_{coh.}$, as previously obtained in Ref. 4 or equivalently from Eq. (10) of this paper by ignoring the factor of 2 in front of $N'_{0_{N\times N}}\Big|_{coh.}$. We observe that the noncoherent symbol synchronizer performs almost as well as the coherent one at high SNR (where the $S\times N$ noise dominates over the $N\times N$ noise) whereas at low SNR (where the $N\times N$ noise dominates over the $S\times N$ noise) there is a more significant degradation of the former relative to the latter. Next, as was the case for the coherent symbol synchronizers, the noncoherent cross-spectrum scheme with half-symbol delay provides an improvement in performance over the filter and square law scheme when

[8] These results were not explicitly given in Ref. 4 but have been independently derived here after considerable manipulation and integral evaluation.

implemented with the optimum value of bandwidth-time product R. Furthermore, although the cross-spectrum schemes exhibit a dependence on the bandwidth-time product for all values of α, this dependence is considerably reduced by the use of a half-symbol delay, particularly when compared with that for $\alpha = 0$.

To explain the much slower roll-off of the squaring loss performance with R for the half-symbol delay case, we reason as follows. In the limit of large low pass filter bandwidth (theoretically no filtering at all), when $\alpha = 0$ the signal component of the output of the delay and multiply circuit (equivalent to a squaring operation in this case) is a squared NRZ waveform which simply is a constant equal to unity and as such does not contain a harmonic at $1/T$. This is born out by the fact that the normalized signal power of the harmonic at $1/T$ as given by $|C_1|^2$ in (11) is equal to zero in the limit of $R \to \infty$. On the other hand, in the same limit with $\alpha = 0.5$, the output of the delay and multiply circuit randomly alternates between a ± 1 square wave at the data rate and a $+1$ constant. The average of these two waveforms is a unipolar (0,1) square wave at the data rate whose Fourier series expansion clearly contains a nonzero harmonic at $1/T$. Once again this is born out by the fact that using (12), in the limit of $R \to \infty$ and $E_s/N_0 \to \infty$ we have $|C_1|^2 = 1/\pi^2$. Since, for large R, the $N'_{0_{N\times N}}\big|_{coh.}$ term dominates over the $N'_{0_{S\times N}}\big|_{coh.}$ and since for $\alpha = 0$ and $\alpha = 0.5$ they both have the same behavior (except for a factor of two smaller for the latter), then when taking ratio of $|C_1|^2$ to the sum of $N'_{0_{S\times N}}\big|_{coh.}$ and $N'_{0_{N\times N}}\big|_{coh.}$, the squaring loss for the half-symbol delay case will decay with R much less rapidly than for the zero delay (squaring) case.

It is now of interest to compare the performance of the noncoherent cross-spectrum symbol synchronizers to that of the coherent DTTL whose squaring loss is given by [1,2]

$$S_L = \frac{2\left[\operatorname{erf}\left(\sqrt{\frac{E_s}{N_0}}\right) - \frac{\xi}{2}\sqrt{\frac{E_s/N_0}{\pi}}\exp\left(-\frac{E_s}{N_0}\right)\right]^2}{\xi\left\{1+\frac{\xi}{2}\left(\frac{E_s}{N_0}\right) - \frac{\xi}{2}\left[\frac{1}{\sqrt{\pi}}\exp\left(-\frac{E_s}{N_0}\right) + \sqrt{\frac{E_s}{N_0}}\operatorname{erf}\left(\sqrt{\frac{E_s}{N_0}}\right)\right]^2\right\}} \tag{13}$$

where ξ is the so-called "window width", i.e., the duration of integration across the symbol transition in the quadrature arm. Figures 5a and 5b are plots of the squaring loss given by (13) versus E_s/N_0 in dB and for comparison the optimum (with respect to choice of R) squaring loss for the coherent and noncoherent cross-spectrum schemes corresponding to $\alpha = 0$ and $\alpha = 0.5$ respectively. In the case of Fig. 5a, we observe that, regardless of its window width, the DTTL outperforms the noncoherent cross-spectrum (filter and square) scheme over the entire range of SNR illustrated. On the other hand when compared to the coherent cross-spectrum scheme, for sufficiently large window width, the DTTL performance will suffer a degradation at low values of SNR. This should not be surprising since as mentioned earlier in the chapter, the DTTL is derived from a high SNR approximation to the MAP symbol synchronizer which itself is motivated by the MAP estimation approach only in the limit of infinitesimally small

window width.[9] With reference to Fig. 5b, we observe that the performance of the coherent cross-spectrum scheme is quite competitive with that of the DTTL having a window width $\xi = 0.5$, and even the noncoherent cross-spectrum scheme can slightly outperform this DTTL at high SNR. As the window width is increased beyond a value of one-half, the cross-spectrum symbol sync schemes will clearly outperform the DTTL over the entire range of SNRs. While it is difficult analytically to obtain the limiting behavior of the cross-spectrum schemes when E_s/N_0 approaches infinity, it can be shown numerically that for both the noncoherent and coherent versions, the optimum value of R is approximately equal to 1.1 and the accompanying value of squaring loss is 6.84 dB.

Conclusions

The results obtained in this paper suggest an alternative to the conventional means of first obtaining carrier sync followed by coherent symbol sync and then iterative handshaking between the two that under certain circumstances can also lead to improved performance.

References

1. M. K. Simon, "An analysis of the steady-state phase noise performance of a digital data-transition tracking loop," *ICC '69 Conf. Rec.*, Boulder, CO, June 1969, pp. 20-9–20-15. Also see, *JPL Technical Report 900-222*, Jet Propulsion Laboratory, Pasadena, CA, November 21, 1968.
2. W. C. Lindsey and M. K. Simon, *Telecommunication Systems Engineering*, Prentice-Hall, Inc., Englewood Cliffs, NJ, 1973. Reprinted by Dover Press, 1991.
3. J. Holmes, "Tracking performance of the filter and square bit synchronizer," *IEEE Trans. on Commun.*, vol. COM-28, no. 8, August 1980.
4. R. D. McCallister and M. K. Simon, "Cross-spectrum symbol synchronizer," *ICC'81 Conf. Rec.*, 1981, pp. 34.3.1–34.3.6.

[9] The window width, ξ, of the DTTL corresponds to the approximation of the derivative of an NRZ pulse at a transition point in the data stream, namely, a delta function, with a finite width rectangular pulse. Thus, the validity of the approximation, as well as the tracking performance of the closed loop DTTL, monotonically improves as the window width becomes smaller and smaller. However, while in principle the MAP approach suggests an infinitesimally window width, in practice there is a lower limit on its value since the width of the tracking region is directly proportional to ξ. Thus, if the window width is made too small, the ability of the loop to remain in lock will severely diminish. The choice of window width is determined by the condition $\sigma_\lambda << \xi$.

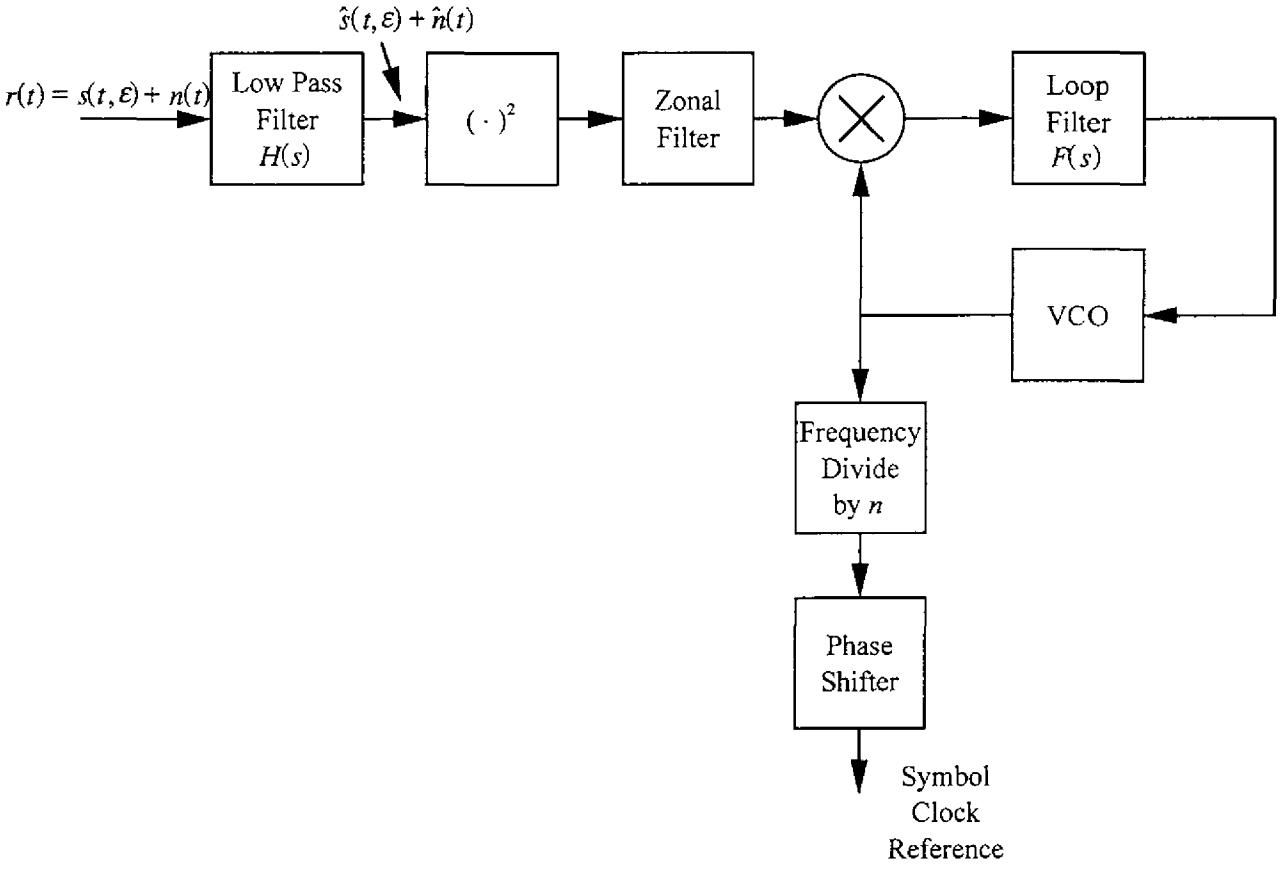

Fig. 1. Filter and Square Symbol Synchronizer

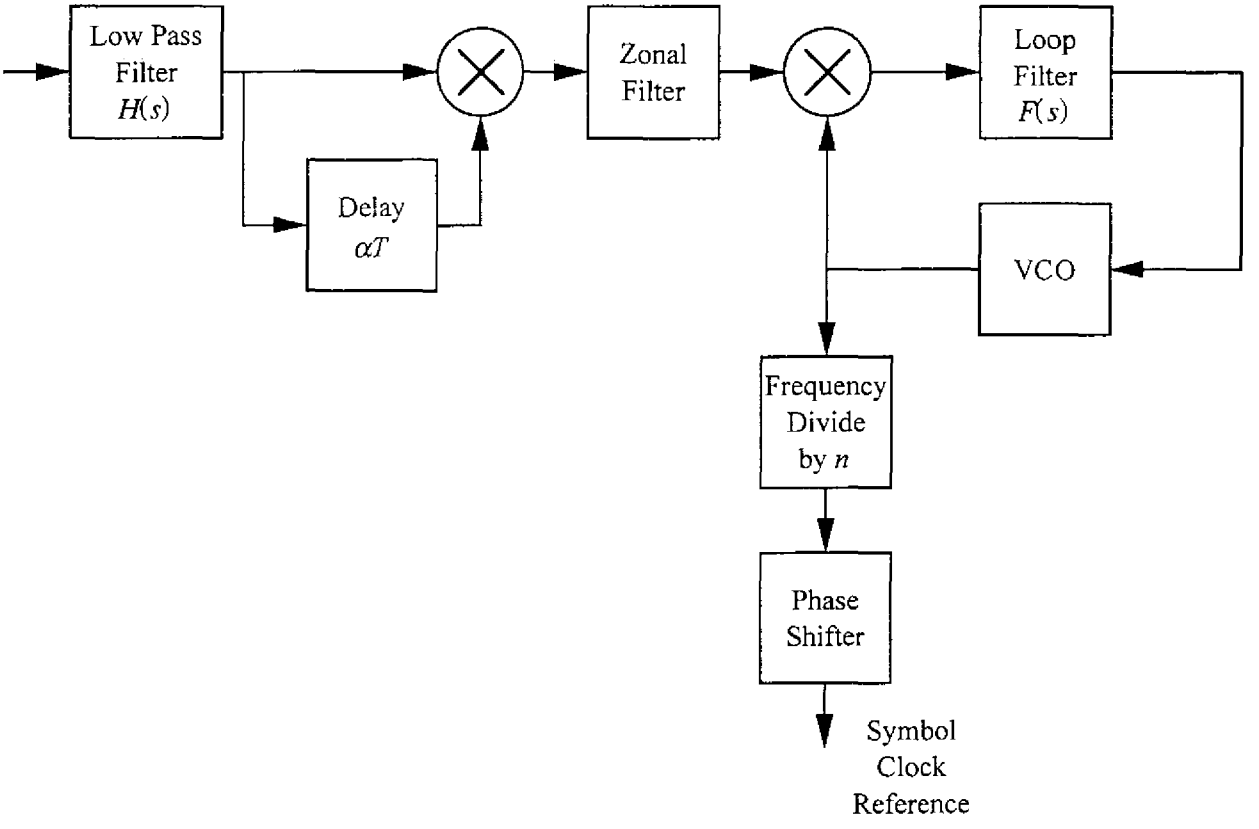

Fig. 2. Cross-Spectrum Symbol Synchronizer

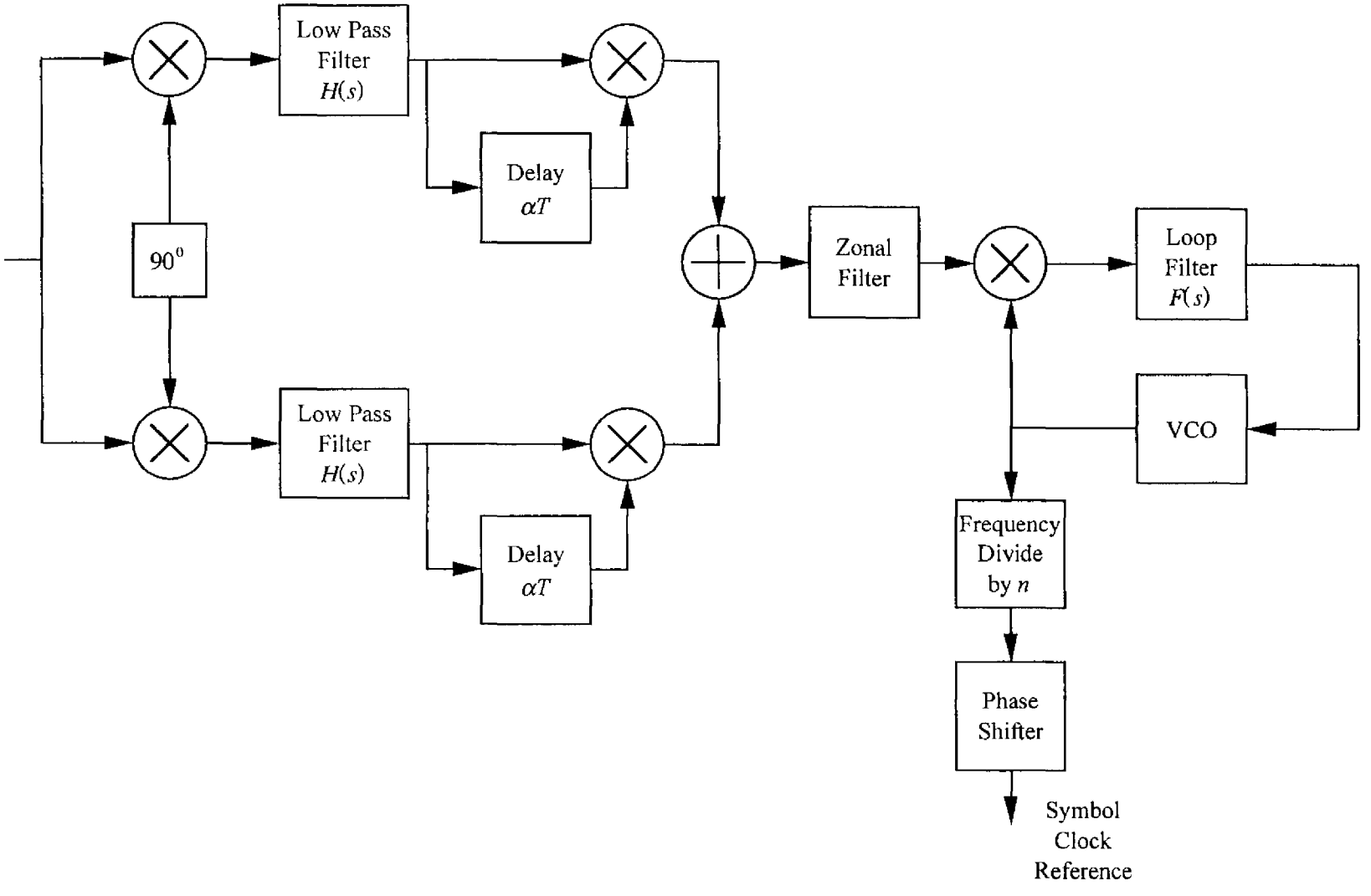

Fig. 3. Noncoherent Cross-Spectrum Symbol Synchronizer

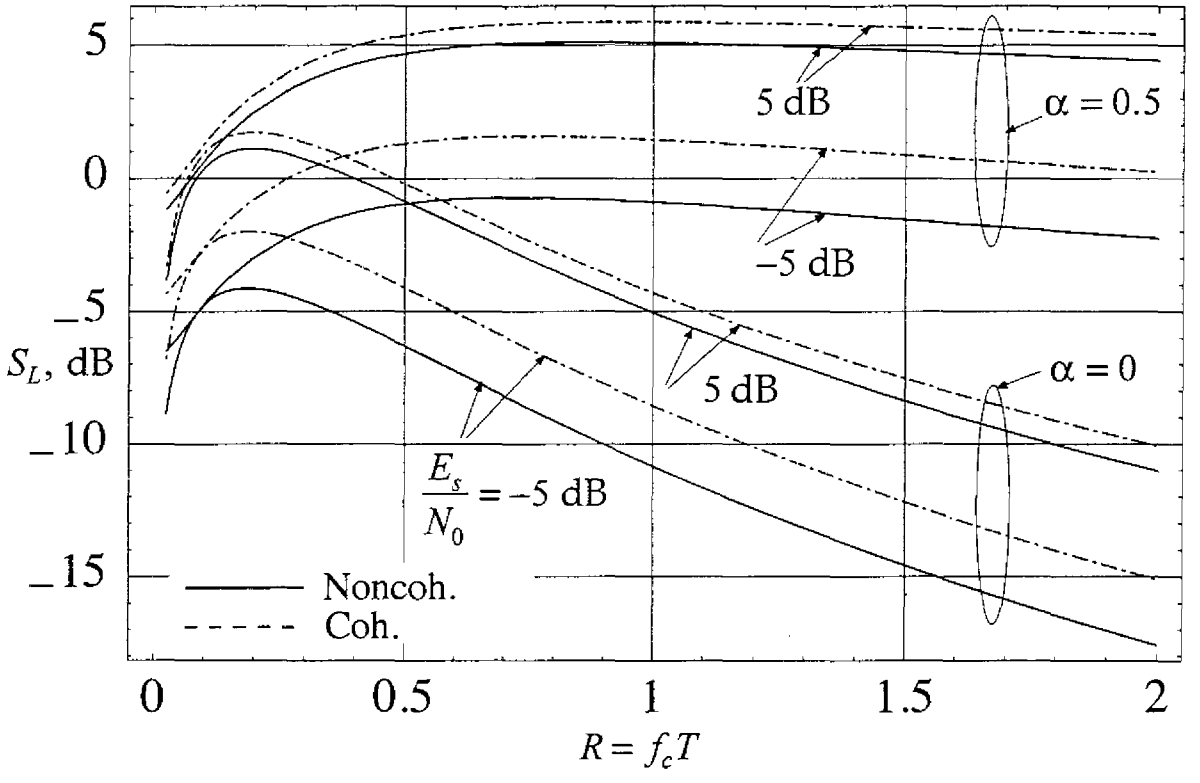

Fig. 4. Squaring loss performance of noncoherent and coherent cross-spectrum symbol synchronizers

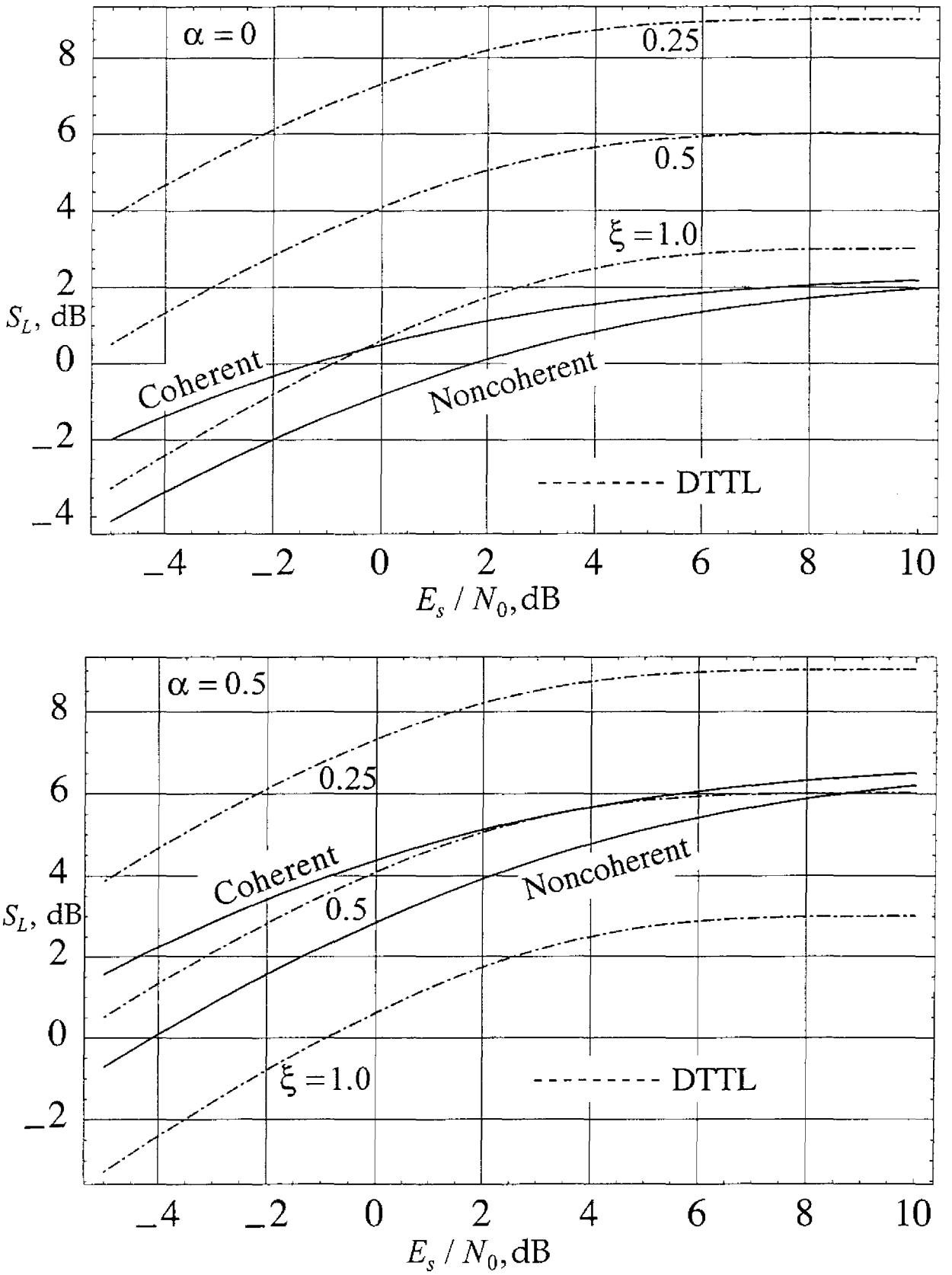

Fig. 5. A comparison of the squaring loss performance of noncoherent and coherent cross-spectrum symbol synchronizers with that of the DTTL: (a) α=0, (b) α=0.5.